

The flight of impact craters based on paleo-positions and its unrestrained latitudinal distribution

James S¹, Saranya R¹, Aneeshkumar V¹, Indu GK¹, Devika P¹, and Sajinkumar KS¹

¹University of Kerala

November 21, 2022

Abstract

Earth's impact craters were analyzed to know the paleo-positions, distance and displacement they have undergone due to plate tectonics. Further, we have verified whether there is any selective distribution across the latitudinal segments. This was achieved through GPlates, a tectonic reconstruction model. The results are intriguing with several craters travelled across the globe. The oldest crater studied was Beaverhead, which travelled from southern to northern hemisphere covering ~39,289 km in 900Ma but with shorter displacement of ~8467km. On the other hand craters like Jänisjärvi and Suvasvesi South have travelled longer distances (27,781 and 29,050km, respectively) and have the distinction of being the most displaced craters (17,400 and 16,988km, respectively). Similarly the paleo-position and the distance as well as displacement for all the craters were recreated. The latitudinal dependency was also studied. Being a planet with varying land area during different geological ages, calculating area is an arduous task. The area of the equal latitudinal segments, viz. 0-30{degree sign}, 30-60{degree sign} and 60-90{degree sign}, were calculated for the respective number of times of impact crater events and compared with the total land area. Results showed that the first two segments have equal crater frequency whereas the polar segment has lesser frequency and we attribute to plates like Antarctica that remained in polar region throughout the Earth history are less explored owing to harsh climatic conditions. These results are compared to that of the Moon and Mars. This reveals that there is a non-selective distribution of impact craters across latitudinal segments.

Hosted file

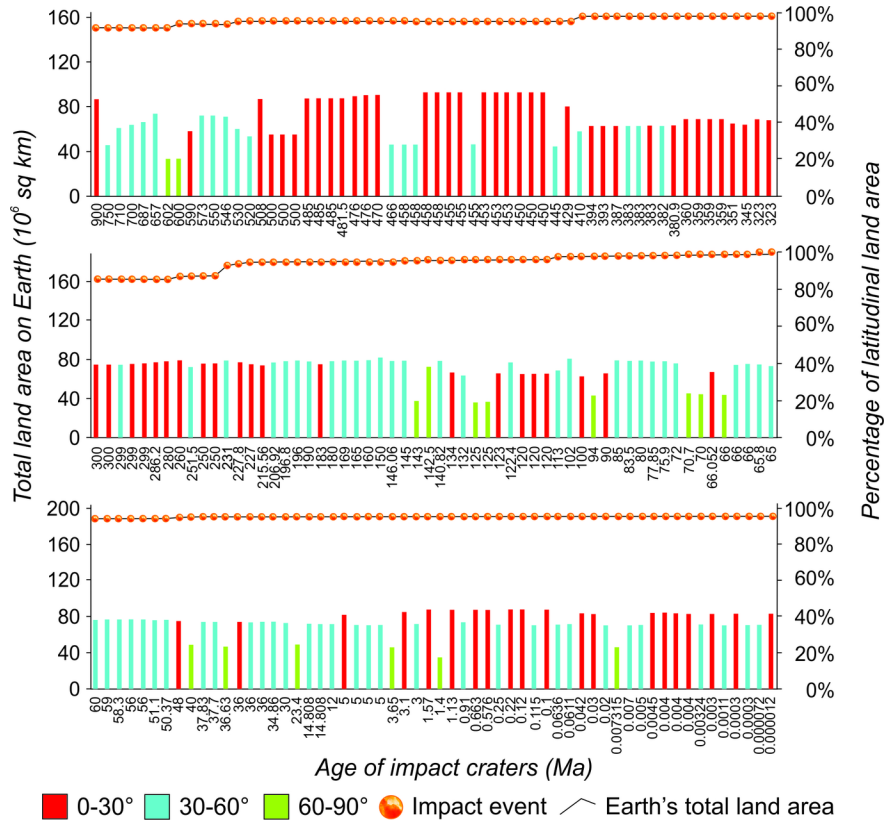
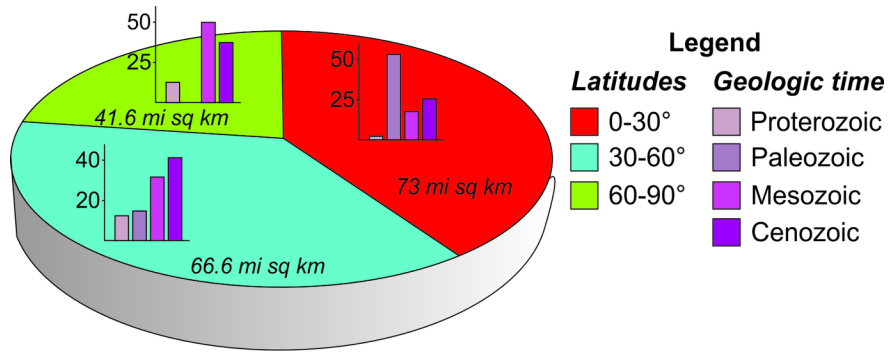
table 1.docx available at <https://authorea.com/users/528315/articles/596843-the-flight-of-impact-craters-based-on-paleo-positions-and-its-unrestrained-latitudinal-distribution>

Hosted file

table 2.docx available at <https://authorea.com/users/528315/articles/596843-the-flight-of-impact-craters-based-on-paleo-positions-and-its-unrestrained-latitudinal-distribution>

Hosted file

table 3.docx available at <https://authorea.com/users/528315/articles/596843-the-flight-of-impact-craters-based-on-paleo-positions-and-its-unrestrained-latitudinal-distribution>



Abstract

23
24
25
26
27
28
29
30
31
32
33
34
35
36
37
38
39
40
41
42
43
44

Earth's impact craters were analyzed to know the paleo-positions as well as the distance and displacement they have undergone due to plate tectonics. Further, we have verified whether there is any selective distribution across the latitudinal segments. This was achieved through GPlates, a tectonic reconstruction model. The results are intriguing with several craters travelled across the globe. The oldest crater studied was Beaverhead, which travelled from southern to northern hemisphere covering ~39,289 km in 900Ma but with shorter displacement of ~8467km. On the other hand craters like Jänisjärvi and Suvasvesi South have travelled longer distances (27,781 and 29,050km, respectively) and have the distinction of being the most displaced craters (17,400 and 16,988km, respectively). Similarly the paleo-position and the distance as well as displacement for all the craters were recreated.

The latitudinal dependency was also studied. Being a planet with varying land area during different geological ages, calculating area is an arduous task. The area of the equal latitudinal segments, viz. 0-30°, 30-60° and 60-90°, were calculated for the respective number of times of impact crater events and compared with the total land area. Results showed that the first two segments have equal crater frequency whereas the polar segment has lesser frequency and we attribute to plates like Antarctica that remained in polar region throughout the Earth history are less explored owing to harsh climatic conditions. These results are compared to that of the Moon and Mars. This reveals that there is a non-selective distribution of impact craters across latitudinal segments.

45 **Keywords:** Impact craters, GPlates, paleo-position, latitudinal dependency, plate
46 tectonics

47 1 INTRODUCTION

48 Impact cratering is one of the most fundamental processes of the Solar System
49 (*Shoemaker 1983; French 1998; Osinski and Pierrazo 2013; Schmieder and Kring*
50 *2020*). The existence and importance of meteorite impact events on the Earth, which
51 was not considered an important terrestrial geologic process earlier, has now been
52 generally recognized and accepted as of significance (*Marvin 1986, 1990, 1999; Hoyt*
53 *1987; Mark 1987; French 1990b, 2004; Grieve 1991, 1998; Grieve and Shoemaker*
54 *1994; Reimold 2003; Reimold and Koeberl 2008*) owing to its role in shaping the
55 planetary surface by forming large circular geological structures, major crustal
56 deformations and generation of large volume of igneous rocks (*French and Koeberl*
57 *2010; Li et al., 2018*). Even the formation of the Moon is described by a ‘Giant Impact
58 Hypothesis’ when the proto-Earth, called ‘Gaia’, and a Mars-sized asteroid called ‘Theia’
59 collided and the ejected materials aggregated to form the Moon, approximately 4.5
60 billion years ago (*Daly 1946; Hartmann and Davis 1975; Cameron and Ward 1976;*
61 *Cameron & Benz 1991; Canup and Asphaug 2001*). Meteorite impact events also
62 resulted in the generation of important economic mineral and hydrocarbon deposits
63 such as Sudbury (Canada), Ternovka (Ukraine), Carswell (Canada), Redwing Creek
64 (USA), Siljan crater (Sweden) and many more (*Masaitis 1992*). Huge impact events also
65 had catastrophic effects leading to the mass extinction of several species on Earth
66 (*French and Koeberl 2010*) with the mostdevastating one being the mass extinction
67 event at the Cretaceous-Tertiary (K/T) boundary around 65 Ma due to the impact at

68 Chicxulub, Mexico (*Alvarez et al. 1980; Schulte et al. 2010*). Some views consider
69 meteorite impacts as the triggering factor for the commencement of plate tectonics
70 (*Sears and Alt 1992; Tianfeng et al. 1997*).

71 Thus, identifying and characterizing impact craters have paramount importance
72 in understanding several global geological processes (*Keerthy et al. 2019*). Yet, in all
73 crater related studies, be it either solely based on craters and associated features or
74 results derived with craters as the primary focus, the current geographic positions are
75 used. This is despite plate tectonics having forced these craters to chart an itinerary
76 through different latitudinal and longitudinal waypoints from their paleo-positions before
77 ephemerally mooring at the current positions. Plate tectonics not only made the journey
78 of craters possible, but also obliterated and destroyed several of them, leaving only ca.
79 200 impact craters on Earth. This rarity contrasts to the the presence of numerous
80 craters on other terrestrial bodies like Moon and Mars, ranging in size from less than a
81 meter to hundreds of kilometers in diameter and ages spanning different time periods.
82 Not only plate tectonics, but weathering, erosion and deposition, have all eroded and/or
83 sepulchered many of the earth impact craters. Hence an understanding of the paleo-
84 position of the impact crater, i.e., the geographical graticule at the time of an impact
85 crater's formation, and its journey from its paleo-position to the current position is
86 essential in gaining a better understanding of several global geological phenomena and
87 possibly alternative theories to explain them.

88 This study thus is an attempt to decipher the position of the earth impact craters
89 at the time of their formation and to elucidate the journey it has undergone since then.
90 The paleo-position of the terrestrial impact craters was determined using a cross-

91 platform plate tectonic geographic information system (GIS), called GPlates, that
92 enables an interactive manipulation of plate tectonic reconstructions (*Müller et al. 2018*).
93 Based on the paleo-reconstruction, an effort has also been made, wherein the position,
94 time and size were compared to understand the latitudinal distribution of impact craters,
95 to know whether any latitude-dependency for meteorite impact events exists. A
96 comparative study on the number and latitudinal distribution of impact craters on the
97 Lunar and Martian terrain is also done, thereby quantifying the cosmic impact events to
98 study its effects on different planetary settings.

99 Literature review on impact craters reveal that only a few studies have been done
100 using the paleo-positions and also in latitudinal-dependency, but they differ from the aim
101 and scope of the present study. *Kresák's (1964)* work is the first available literature
102 wherein he studied the latitudinal variation of meteor shower using 24 major shower
103 events and with some sporadic background. *Halliday (1964)* was the first to attempt a
104 study exclusively on impact events and concluded that the meteorite falling on the earth
105 is moderately dependent upon latitude. *Thackeray et al. (2006)* studied the latitudinal
106 distribution of impact craters based on crater paleo-positions by correcting the apparent
107 effect of plate tectonics, though the exact paleo-coordinates of impact craters have not
108 been provided. *Wieczorek and Le Feuvre (2008)* studied both the impact flux and
109 cratering rate as a function of latitude using a model distribution of planet crossing
110 asteroids and comets for all the terrestrial planets wherein they concluded a non-
111 uniform impact cratering mechanism. Crater paleo-position was utilized by *Spray et al.*
112 *(1998)* and *Telecka and Matyjasek (2011)* to study the catena events. Seldom studies,
113 like *Spray et al. (1998)* and *Telecka and Matyjasek (2011)*, been successful in

114 reconstructing the exact paleo-coordinates, but with limited geological time-scale. Thus
115 our study differs from the above mentioned works, by studying the paleo-positions of all
116 the earth impact craters and its journey, latitudinal dependency, and its comparison with
117 the Moon and the Mars.

118 **2 MATERIALS & METHODS**

119 **2.2 Database of impact craters on Earth, Moon and Mars**

120 The list of confirmed impact craters of Earth is mainly collected from the Earth
121 Impact Database (<http://www.unb.ca/passc/ImpactDatabase/>), developed and
122 maintained by the Planetary and Space Science Centre, University of New Brunswick,
123 Canada, as well as from several published literatures. Today the total number of
124 confirmed impact craters on Earth comes around 200 in number. Of these structures,
125 the paleo-position reconstruction has been carried out for craters younger than 1100 Ma
126 due to constraints associated with GPlates plate motion model.

127 The Lunar impact database was obtained from *Robbins (2019)* that is freely
128 available in the website of United States Geological Survey's (USGS) National
129 Aeronautics and Space Administration (NASA) Planetary Data System (PDS)
130 ([https://astrogeology.usgs.gov/search/map/Moon/Research/Craters/lunar_crater_data-
131 se_robbins_2018](https://astrogeology.usgs.gov/search/map/Moon/Research/Craters/lunar_crater_database_robbins_2018)). This database presents a comprehensive record of all the craters
132 with diameter greater than 1-2 km. With 2,033,574 number of identified Lunar impact
133 craters, *Robbins (2019)* presents the largest database than any other previously
134 published data by more than a factor of 10.

135 Martian global crater database, prepared by *Robbins and Hynek (2012)*, is used
136 for the present study. This was also downloaded from the USGS' NASA PDS

137 ([https://astrogeology.usgs.gov/search/details/Mars/Research/Craters/RobbinsCraterDat](https://astrogeology.usgs.gov/search/details/Mars/Research/Craters/RobbinsCraterDatabase_20120821/zip)
138 [abase_20120821/zip](https://astrogeology.usgs.gov/search/details/Mars/Research/Craters/RobbinsCraterDatabase_20120821/zip)). This database is composed of a total of ~ 632,000 craters
139 including those with diameters down to ~ 0.5 km. The global database of Martian impact
140 craters with diameter >1-2 km is used for the present study with a record of 384,343
141 craters. They provided the extensive database of Martian impact craters, identified
142 manually by using daytime infrared image mosaic by Thermal Emission Imaging System
143 (THEMIS Day IR) aboard the 2001 Mars Odyssey NASA spacecraft; Viking Mars digital
144 image model 2.1 (Viking MDIM 2.1) and Context Camera (CTX) mosaics from Mars
145 Reconnaissance Orbiter (MRO); and Mars Orbiter Laser Altimeter (MOLA) data from
146 the Mars Global Surveyor mission.

147 **2.2 Elucidating the paleo-position of Earth impact craters using GPlates**

148 Paleo-position and latitudinal distribution of Earth impact craters are mainly
149 generated by the plate tectonic reconstruction models offered by the GPlates 2.2.0
150 software. GPlates, a free desktop software that can be downloaded from
151 www.gplates.org and designed for interactive visualization of plate tectonics, was
152 developed by an international team of scientists and software developers at the
153 EarthByte Project (www.earthbyte.org) in the School of Geosciences at the University of
154 Sydney, the Division of Geological and Planetary Sciences (GPS) at Caltech, and the
155 Centre for Geodynamics at the Norwegian Geological Survey (NGU) (*Boyden et al.*
156 *2011*). GPlates provides a compiled output of GIS-based interactive plate tectonic
157 reconstructions, and raster data visualization. The application of GPlates, both in
158 visualization and manipulation of plate-tectonic reconstructions and associated data
159 through geological time, enables its usage in finding the paleo-position of terrestrial

160 impact craters distributed over all the continents. The major advantages of using
161 GPlates include handling and visualizing data in a variety of geometries and formats,
162 link plate kinematics to geodynamic models, which serve as an interactive client in a
163 grid-computing network and facilitate the production of high quality paleo-geographic
164 maps. GPlates facilitate the reconstruction of tectonic plates for a single instant in
165 geological time or animate a sequence of reconstructions over a user-specified
166 geological time-period (*Boyden et al. 2011*). The present study on the paleo-position of
167 impact craters has primarily made use of the PALEOMAP PaleoAtlas for GPlates by
168 *Scotese (2016)* grouped under the paleogeography portal of the GPlates resource
169 (<https://www.earthbyte.org/category/resources/data-models/paleogeography/>). It is
170 composed of 91 paleo-geographic maps spanning the Phanerozoic and late
171 Neoproterozoic. PaleoAtlas database is designed up to only 1100 Ma and therefore in
172 the present study craters of age less than 1100 Ma were selected and that come only
173 174 craters. The technical constraints limit the reconstruction of plate movements
174 further backwards to its exact origin and would probably be overcome in the near future.

175 The PaleoAtlas can be directly loaded into GPlates as a time-dependent raster
176 file. For the present study PALEOMAP Global Plate Model has been used, which
177 consists of three separate files -PlateModel, -PlatePolygons, and -PoliticalBoundaries.
178 These files are opened and exported from GPlates to ArcGIS for plotting all the impact
179 craters on its respective plates. The map files of impact craters have been exported into
180 a shapefile suitable for working in the GPlates. The shapefile that consist the craters is
181 opened in the GPlates as a separate layer.

182 **2.3 Ascertaining ages to impact craters**

183 The major constrain faced is in deciding the exact age of impact event as the age
184 determined for the craters comes in different forms like some craters had specific ages
185 (e.g., Spider, Australia with 700 Ma; *Flamini 2019*), whereas some others with minor
186 uncertainties around a specific value (e.g., Lonar crater, India with 0.576 ± 0.047 Ma;
187 *Jourdan et al. 2011*), while some had a range of ages (e.g., Connolly Basin, Australia
188 with ~66 to 23 Ma; *Shoemaker & Shoemaker 1986*), whilst some showed the upper age
189 limit (e.g., Eagle Butte, Canada with <65 Ma; *Grieve 2006*), and some other craters
190 showed only a lower age limit (e.g., Crawford, Australia with >35; *Haines et al. 2005*).
191 Therefore to avoid further confusions, an age, called optimum age, was considered in
192 the present study to compute the paleo-position of the crater, along with distance and
193 displacement recorded by the crater from its original paleo-position. For example,
194 optimum age for Spider was ascertained 700 Ma; Lonar 0.576 Ma; Connolly Basin 66
195 Ma; Eagle Butte 65 Ma and Crawford 35 Ma. Further paleo-positions were also
196 calculated for the secondary and tertiary ages. For example, where $A\pm U$ (A =Age Value
197 and U =Uncertainty Value) is mentioned as the age of the crater, we consider A as the
198 optimum age; while $A+U$ is the secondary age (Upper Age Limit) and $A-U$ is the tertiary
199 age (Lower Age Limit); and if crater's age is in a range such as $A-B/<A-B/\sim A-B$ (where
200 $A>B$), A is the optimum age and B is the secondary age; whereas for craters with ages
201 $<A/\leq A/\sim A$, A is considered as the optimum age as it is the only available age for the
202 crater. Thus, there are uncertainties in the paleo-positions, distance and displacement
203 of the craters. For example, Connolly Basin exhibits the paleo-coordinates of -49.86 and
204 115.04, a distance of 3179.71 km and a displacement of 3041.93 km for the optimum
205 age when compared to paleo-coordinates of -36.92 and 118.28, a distance of 1608.54

206 km and a displacement of 1608.21 km for the secondary age. The uncertainties can be
207 reduced by the availability of more precision dating techniques.

208 In the next step plate IDs have been assigned to each crater for establishing the
209 paleo-position and plate motions are animated according to the desired age of
210 reconstruction. For each crater, plate motions have been reconstructed from the time of
211 its formation to present day. The paleo-position of each crater is determined at the age
212 of formation by zooming to the maximum extent at the preposition of craters. Further the
213 motion path of all the craters have been generated marking the trail of craters; this
214 exercise helps estimate the distance covered by craters as they journeyed to their
215 present day location.

216 **2.4 Dissection of Earth into different latitudinal zones and reclassification of** 217 **impact craters**

218 A little fuzziness was there when the latitudinal division required for the present
219 study had to be selected. Initially the curvature of the arc of the earth at different
220 locations was calculated (Supporting Information 1). But there were no major changes
221 in the curvature at poles and equator. Also the climatic zone classification as Tropic of
222 Cancer and Capricorn as well as Arctic and Antarctic Circles is based on obliquity of the
223 ecliptic. Hence we were prompted to discard the above mentioned two classifications
224 and opt an equal latitudinal distribution classification in which the Earth is divided into
225 three equal latitudinal groups viz., 0° - 30° , 30° - 60° and 60° - 90° (for both Northern and
226 Southern Hemispheres). The reason why an equal latitudinal distribution classification
227 was selected was that it is unbiased in terms of category selection and each category is
228 given the same proportion of the range of values.

229 After plotting the paleo-position of the impact craters in the latitudinal segments,
230 the crater frequency within each latitudinal segment was calculated. This was carried
231 out by estimating the land area within the three respective zones (in order to achieve a
232 true comparison, we focus solely on the land area. Ocean area was excluded as we
233 have few crater records from it) during the impact event. In order to estimate the land
234 area within the zones, Earth is projected by applying Cylindrical Equal Area Projection.
235 In this projection, the latitudes and longitudes are represented as perpendicular straight
236 lines. Even though the meridians are equally spaced, the spacing between consecutive
237 latitude decreases from the equator to poles (higher latitudes). The main advantage of
238 this projection is conservation of area of Earth by retaining the actual dimensions of
239 features on Earth (*ESRI 2015*). Consequently, there is significant distortion of scale,
240 shape, direction and angle from the equator to the poles; making it a non-conformal
241 projection. Irrespective of this we proceed with this projection to acquire area within
242 each latitudinal segment. It is to be noted that all this study is done from 900 Ma (age
243 corresponding to Beaverhead, the oldest crater considered in this study) to the present
244 day.

245 The present total surface area of Earth is 510.1 million sq.km, where the area
246 occupied by present day land and ocean are 148.9 million sq. km. and 361.1 million
247 sq.km, respectively. On categorizing the present area of Earth to three zones, the total
248 area (inclusive of land and ocean) of 0-30° segment is 254.7 million sq. km., 30-60° is
249 186.9 million sq.km and 60-90° is 68.8 million sq.km. While the total area of Earth
250 remains the same in our calculations, the total current land area on Earth computed by
251 shapefiles, imported from GPlates, stand at 190.5 million sq.km and oceans constitute

252 an area of 320 million sq.km. The disparity in actual and computed land and ocean area
253 is associated with the calculation method, where values are retrieved through the
254 summation of area of projected shapefiles, provided in ArcGIS. This method essentially
255 adds the area of oceanic plates like Pacific Plate and oceanic regions of plates like
256 African and South American plates that contain a substantial part of the Atlantic,
257 resulting in additional areas associated with land. For the study, a computed Earth area
258 of 190.5 million sq.km is thus used. On measuring land area of latitudinal zones, areas
259 of oceanic regions are not measured; thereby giving us precise values in these
260 segments for the paleo-positions. The surface area of the Earth is thus downsized to
261 190.5 million sq.km by eliminating the area constituted by oceans (Video file (3 parts) of
262 the entire methodology is shown in supporting information 2).

263 **3 RESULTS**

264 **3.1 Paleo-position and journey of Earth impact craters**

265 Since establishing the first Earth impact crater at Barringer to the present day,
266 the study of terrestrial impact craters has been consequential in providing
267 comprehensive information about several aspects of the planet and the Solar System.
268 But almost all the studies were restricted to the current position of the impact craters,
269 without considering the paleo-position and the journey it has undergone. Therefore,
270 here we done a paleo-tectonic reconstruction of the impact craters and studied the
271 paleo-coordinates, paleo-plates, and the distance travelled as well as the displacement
272 for all the terrestrial impact craters, which was reproduced using GPlates (only the 8
273 oldest craters are shown in Table 1 due to space constrain and the rest in Supporting
274 Information 3).

275 Figure 1 shows the paleo-position as well as the present position of the impact
276 craters. The trails in figure 1 connect the paleo- to the current position and this shows
277 that the terrestrial impact craters are geographically sprawled over all continents with
278 the exception of Antarctica. However, when craters are categorized according to paleo-
279 tectonic plates (Table 1), it can be noted that these 174 craters are contained in only 26
280 tectonic plates (inclusive of micro- and macro-plates) present on Earth. The most
281 extreme case is when a tectonic plate represents the entire continent like Australia,
282 where all craters lie in Australian Plate, whereas Asia form the other end of the extreme,
283 where a comparatively large number of plates constitutes the continent. The Central
284 Honshu, Arabia, Indian Craton, Siberian Craton, North Slope Alaska, Kazakhstan,
285 Indochina and North China Platform plates accommodate the Asian craters. Other
286 major plates like the North American Craton plate contain more than 80% of total crater
287 belonging to North America, while minor plates like Baffin Islands, Yucatan, North Slope
288 Alaska and Piedmont-Florida contain the remaining craters. In South America, the
289 South American Craton contains 73% of craters while the minor Parana Basin plate
290 constitutes the rest of the craters. The African craters are present in 3 plates namely,
291 African Craton, Northwest African and Northeast African Plates. Similarly, European
292 craters are found in North European Craton and Eurasian plates, along with Central
293 Europe and Central Svalbard plates.

294 The journey of impact craters were derived by ascertaining a single age to crater
295 (which we call here as optimum age), while the age of craters are mentioned with
296 uncertainties, like any other geological samples. In this study the single age,
297 represented by the optimum age, was substituted to all the paleo-positions of the

298 craters. Regarding the journey of the craters, obviously the older craters tend to cover
299 greater distance from respective paleo-positions to reach current positions than the
300 younger craters as plates containing older craters are subjected to longer durations of
301 plate tectonics (Table 1) (paleo-position, distance and displacement covered by the
302 impact craters with respect to the secondary and tertiary ages for all the craters are
303 given in the supporting information 4 and 5, respectively). That being said, it is to be
304 noted that the youngest of craters, like Carancas, Sikhote Alin, Sobolev, Wabar,
305 Whitecourt, Dalgaranga, Kallijärv, Campo Del Cielo, Veevers, Kamil and Luna, hardly
306 describe any movement and therefore, there is not significant change in their
307 proposition. Beaverhead in the USA, the oldest crater in the present study with an age
308 of 900 Ma, covers maximum distance from its paleo-position to current position, valued
309 at 39,289.44 km. With the exception of Beaverhead, there are 3 more craters that have
310 traveled distances greater than 30,000 km, which are Ramgarh, India (750 Ma), Spider,
311 Australia (700 Ma) and Strangways, Australia (657 Ma). The least distance is covered
312 by Ilumetsä (0.007 Ma) at 40.3 m, apart from the above mentioned 11 youngest craters.
313 The distance covered by craters progressively increases from Ilumetsä to Beaverhead.
314 Though distance traveled increases with age, it also depends on crater position on their
315 respective plate and plate velocities. Therefore, craters with similar age might not record
316 similar distance. For example the African craters Gweni-Fada and Aorounga, belonging
317 to Northeast African Plate, with both have primary age 383 Ma, covers similar distance
318 at 11929.38 km and 12033.63 km, respectively. Whereas, the 383 Ma Piccaninny
319 Crater of Australia covered 19114.27 km and North American crater Flynn Creek with

320 an age of 382 Ma covered 15,592.88 km from its paleo-position. Therefore, distance
321 helps in quantifying the path of a crater since its formation.

322 Displacement is another important parameter. It will be difficult to rely on distance
323 covered (derived from motion path) by a crater to give a simplistic trend in position
324 change of crater as path traversed by a crater changes at several intervals. So, we use
325 displacement to accomplish the same. Unlike distance, which increases with age of the
326 crater, displacement does not show any such correlation and is random. Notably,
327 distance and displacement values are the same for younger craters with ages <5 Ma
328 and are also the same for craters up to age <35 Ma, but beyond 35 Ma, large variations
329 are visible. Jänisjärvi, Russia, has recorded maximum displacement of 17399.78 km
330 (Fig. 2), closely followed by Suvasvesi South, Finland, with 16987.58 km. Many of
331 European craters have moved from the Southern Hemisphere all the way to the
332 Northern Hemisphere, producing displacement values greater than 10,000 km, such as
333 Granby, Lumparn, and Sääksjärvi to name a few. After European craters, Australian
334 craters show significant displacement by moving South from Western Hemisphere
335 through Eastern Hemisphere. Spider Crater has a displacement greater than 10,000 km
336 in Australia. Older aged craters need not show greater displacement than younger
337 craters and this can be exemplified by two North American craters, namely Beaverhead
338 (900 Ma) and Flynn Creek (382 Ma), where Beaverhead is displaced 8467.53 km and
339 Flynn Creek is displaced 9858.21 km. Though the general path followed by both is
340 northward, Flynn Creek is positioned at higher latitude than Beaverhead, by virtue of the
341 different tectonic plates these belong to.

342 **3.2 Dissection of Earth into different latitudinal zones and reclassification of**
343 **impact craters**

344 The paleo-positions of craters are then classified into one of these three divisions
345 (0° - 30° , 30° - 60° and 60° - 90°). Through this we intend to study crater frequency for each
346 latitudinal class. Several studies have ascertained that meteorite and impact fluxes
347 witness notable variation with geographic latitude (*Halliday, 1964; Halliday and Griffin,*
348 *1982; Feuvre and Wieczorek, 2008; Evatt et al., 2020*). The above mentioned studies
349 incorporate a large number of influx events and varied components for analyzing
350 latitudinal variation but the fairly small numbers of terrestrial impact craters restrict our
351 capability of replicating the exact set of results. Hence, we attempt to draw a moderate
352 comparison of our results with the earlier studies.

353 The land area contained in each latitudinal zone at the time of formation of
354 impact craters is calculated (only the 8 oldest craters are shown in Table 2 due to space
355 constrain and the rest in Supporting Information 6). Figure 3 shows the entire latitudinal
356 segments together with 174 craters with respect to area and age. The latitudinal
357 segment 0 - 30° constitutes 78 of 174 craters with a diversified age: the oldest crater
358 being Beaverhead (900 Ma) and youngest is Carancas (0.000012 Ma). Between the two
359 age limits, land areas reached their peak in two time periods, namely Ordovician period
360 and Pliocene–Holocene epochs. The average area of this zone, from 900 Ma to present
361 day, is 73 million sq.km. Therefore, a crater is present in every 0.94 million sq.km. area
362 which makes for 1.28% land area of the segment. Proterozoic contributes only two
363 craters in this zone while the remaining 76 craters were added in the Phanerozoic;
364 where Paleozoic with 42 craters contributing over 55% of craters, followed by Cenozoic

365 having 20 craters (26.3%) and Mesozoic recording 14 craters (18.4%)(Fig.4). The 30-
366 60° segment received the maximum number of craters with 80. The most recent crater
367 in this zone is Sikhote Alin aged 0.000072 while the oldest crater is Ramgarh, aged 750
368 Ma. The variation of land area proportion depicts a hither and thither pattern in the 30-
369 60° latitudinal segment. Land area increases from 27% to 44% from Tonian to
370 Cyrogenian period, after which it consistently decreases till late Ordovician (27%). The
371 average area of this zone computed from 750 Ma to present day is 66.6 million sq.km.,
372 where 0.83 million sq.km. area contains a crater. Out of the total 80 craters, 8 (10%)
373 were formed in Proterozoic and 72 craters (90%) in Phanerozoic; wherein, Paleozoic
374 has 12 craters (15%), Mesozoic 26 craters (32.5%) and Cenozoic accounts for 34
375 craters (42.5%) (Fig.4). The 60-90° latitudinal segment has a relatively small number of
376 craters, probably giving a rather incomplete picture for the segment. The average area
377 of the segment stands at 41.6 million sq.km. Phanerozoic contains the bulk of the crater
378 count with 14 craters (87.5%) and Proterozoic has 2 craters (12.5%). Here, 8 craters
379 (50%) formed in Mesozoic and 6 craters (37.5%) in Cenozoic (Fig.4). The oldest crater
380 formed is Sääksjärvi at 602 Ma, which is closely followed by Saarijärvi at 600 Ma, after
381 which no craters are recorded till Mjølner at Cretaceous (143 Ma). Macha crater formed
382 at 14 Ma is the most recent crater.

383 The size distribution of impact craters in these three segments was also studied.
384 Only with 16 craters, 60-90° latitudinal segment has the highest average diameter of
385 24.08 km owing to the presence of three bigger craters viz. Popigai (100 km), Kara (65
386 km) and Tookoonooka (50 km). This latitudinal segment was followed by 0-30° segment
387 with 14.84 km average diameter and this segment was characterized by five bigger

388 craters namely, Chicxulub (180 km), Manicougan (100 km), Acraman (90 km),
389 Beaverhead (60 km) and Charlevoix (54 km). 30-60° latitudinal segment has the
390 comparatively smaller average diameter with 12.73 km. Puchezh-Katunki (80 km),
391 Morokweng (70 km) and Kara-Kul (52 km) are the bigger craters in this latitudinal
392 segment.

393 **4 DISCUSSION**

394 The paleo-reconstruction of the modest number of Earth impact craters using
395 GPlates suggests that all the craters, barring the youngest ones, was in different
396 geographical graticule and has travelled several kilometers. The absence of craters
397 between 1100 and 900 Ma makes it difficult to generate a coherent conclusion for older
398 craters. The haphazard movement of plates across the globe also has made the
399 craterstravel from eastern to western hemisphere and vice-versa as well as northern to
400 southern hemisphere and vice-versa. A few of the craters that transitioned between
401 western and eastern hemispheres are Acraman, Spider, Strangways, Lockne, Mizara,
402 Kardla and Malingen; while Kentland, Saqqar, Beaverhead, Suvasvesi South, Janisjarvi
403 and Acraman are a few examples that depict movement between northern and southern
404 hemispheres. Similarly the craters that have formed at similar time have shown differing
405 movements that give indications on which part of the plate moved very fast and which
406 part has movedless. At 458 Ma, the craters Calvin and Brent formed on the North
407 American Craton. Calvin covered 329 km more than Brent to reach its current position,
408 indicating that the portion of the North American plate accommodating Calvin traversed
409 faster than the part containing Brent.

410 The three different latitudinal segments viz., 0-30°, 30-60° and 60-90° show
411 different crater frequencies. Though the first two segments show similar frequencies
412 irrespective of the ratio of land they possess, the 60-90° segment has less frequency.
413 The 0-30° segment contributes for the most area among the three segments. The
414 comparatively higher crater frequency in this zone is attributed to this increased surface
415 area. The 30-60° segment accommodates a relatively greater proportion of land area
416 (especially in the Northern Hemisphere), increasing the exposure to impact events. This
417 segment has the highest crater frequency with 46%, even though this segment has less
418 surface area than the 0-30° segment. Of the 16 craters in the 60-90° segment, 11 have
419 formed at latitudes between 60-70° ranges, confirming the inaccessibility of the higher
420 latitudes for crater hunting. Additionally the smaller proportion of continental crust also
421 exposes the lower frequency of impact events in the 60-90° segment. But irrespective of
422 the crater locations in the latitudinal segments, most of the youngest craters identified
423 are from developed nations pointing to the importance given to crater research in these
424 nations.

425 Just to validate the results of the latitudinal dependency of Earth impact craters,
426 we have compared the results with those of the neighboring two terrestrial body viz.
427 Moon and Mars. Selection of these terrestrial bodies are not biased, rather these three,
428 including Earth, form a three end member system: one with active plate tectonics
429 (Earth), one devoid of plate tectonics (Moon) and the other which witnessed plate
430 tectonics initially, but is now a geologically dead planet (Mars). Compared to these two
431 distinct cosmic objects, Earth has only a very small number of confirmed impact craters
432 on its land surface owing to the active surficial geological processes and also due to

433 plate tectonics, which has led to the dynamism of the itinerant Earth across latitudinal
434 zones over time. For example, from 900 Ma to present day, the 0-30° segment has
435 changed from 79.4 million sq.km land area, making for 53% of the total land area on
436 Earth (150.8 million sq.km) and at 0.000012 Ma when the last crater was formed in this
437 segment, it contained 41% of total land with 79 million sq.km out of 190.4 million sq.km.
438 This was overcome by calculating the land area for the respective latitudinal zones for
439 'n' times ('n' represents the number of impact crater events) and summation was done,
440 which was further used to calculate the average land area. The average land area was
441 used to derive a ratio with respect to the total land area of the Earth at that particular
442 time. This ratio was normalized and the frequency of the impact craters was studied
443 (Table 3).

444 The databases of impact craters on Moon and Mars were taken from two
445 different sources. Lunar global impact crater database of *Robbins (2019)* is enriched
446 with a total number of ~2 million craters (Supporting Information 7). The database is
447 particularly composed of 1,296,879 craters having diameter ≥ 1 km, 83,000 having ≥ 5
448 km diameter and 6,972 craters having ≥ 20 km diameters. In the case of Mars some
449 384,343 impact craters with diameters ≥ 1 km were analyzed by *Robbins and Hynes*
450 *(2012)*. Similar to the latitudinal distribution classification applied to the Earth surface,
451 Lunar and Martian surfaces were also classified into three latitudinal groups, viz., 0°-
452 30°, 30°-60° and 60°-90° (for both Northern and Southern Hemispheres). Unlike the
453 terrestrial planetary conditions, there is no scope for determining the paleo-position of
454 lunar craters since there is no change in the location of these craters owing to the
455 absence of plate-tectonics. The paleo-position of Martian impact craters were also not

456 done owing to the limitations in the available reconstruction models for Mars. Therefore
457 the Lunar and Martian impact craters paleo-positions were considered to be the same
458 as of today. Seemingly the geologically dead nature of both Moon and Mars resulted in
459 the preservation of a large number of impact craters across the latitudes, which resulted
460 in the huge difference in impact crater record between Earth, Moon and Mars.

461 The percentage of crater in each latitudinal range shows good correlation
462 between Earth and Moon (Fig. 5), whereas the slightly variable yet promising values
463 obtained for Mars might be the reflection of long-ceased paleo-plate tectonics that once
464 prevailed on the planet (*Sleep 1994; Connerney et al. 1999*). Despite the technical
465 constraints while collecting the database of impact craters on Earth, Moon and Mars the
466 data that we present here shows a fairly greater percentage of impact craters at the
467 equatorial bulge of the planetary bodies. Meanwhile the crater distribution in the polar
468 regions is sparse. In between the equatorial and polar regions, in the 30°-60° range, the
469 percentage of crater distribution is more or less similar for the Earth, Moon and Mars.
470 While the first two latitudinal segments show high frequency, the polar regions shows
471 less frequency for all the three bodies. The lower surface area exposed in the polar
472 region might have resulted in the lower frequency of impact craters in this segment on
473 the Earth.

474 Thus in the present study we were able to bring about the latitudinal dependency
475 of impact crater generation on Earth compared to two other neighboring planetary
476 bodies. Besides, comparative latitudinal dependency of impact cratering events, the
477 paleo-position or the original position of the crater at the time of impact have been
478 traced out using GPlates. The paleo-position of impact craters have been obtained for

479 all the possible ages for a particular crater based on its established age. This gives
480 more robust data for the comparison of impact craters on earth to that of the tectonically
481 dead lunar and tectonically dormant Martian surfaces.

482 **5 CONCLUSIONS**

483 The plate tectonic process has immensely modified the surface of the earth,
484 either constructively or destructively. One such ruined geological feature that has a vital
485 role in elucidating several global geological processes is the meteorite impact craters.
486 Though a fistful of studies have been carried out in the field of impact craters, most of
487 the studies were restricted to the present day geographic position of the impact crater.
488 But these impact craters have travelled along with the lithospheric plates through the
489 process of plate tectonics all across the geological time scale. Hence there is a
490 requirement of understanding the paleo-position of impact craters and the flight they
491 have undergone. And thus this study focuses on these issues. Moreover, the rarity of
492 craters in the polar area also prompted us to study whether there is any latitudinal
493 dependence of the impact craters.

494 With the available capabilities of GPlates, the study was successful in
495 deciphering the paleo-positions of impact craters and the journey they have undertaken
496 since origin through the process of plate tectonics.

497 Being a paleo-reconstruction study, it has its own advantages and limitations.

498 The main advantages of this study are

- 499 i. The vast database generated on the paleo-coordinates, and the distance and
500 displacement the craters have experienced will be robust information that can be
501 used for other studies.

502 ii. In comparison with the two adjacent terrestrial bodies and the random observation
503 of impact craters of differing sizes on different latitudes, it is suggested that impact
504 events are unrestrained by latitudes.

505 iii. The haphazard movement of impact craters, owing to plate tectonics, opens anew
506 avenue for studying the plate tectonic history of the earth.

507 Whereas the major limitations are:

508 i. The geologic age of all the craters has an ambiguity. Hence to eliminate this
509 ambiguity, we have considered the optimum age. So the paleo-position as well as
510 the distance and displacement will also be an approximation.

511 ii. The paleo-position of the craters older than 1100 Ma was not deciphered owing to
512 the limitations of the GPlates and this will be overcome when the model is refined.

513 iii. Projectiles and directions of meteorite fluxes were not attempted as it is beyond the
514 scope of our present work.

515 **Acknowledgments**

516 James acknowledges the University of Kerala whereas Saranya thanks the
517 Kerala State Council for Science and Technology (KSCSTE) for funding their PhD and
518 Aneeshkumar thanks the Council for Scientific and Industrial Research (CSIR). The
519 entire work was carried out at the Laboratory for Earth Resources Information System
520 (LERIS) housed at the Department of Geology, University of Kerala. LERIS is a
521 collaborative initiative of Indian Space Research Organization and University of Kerala.
522 Important data pertaining to this study is uploaded in Figshare repository (DOI:
523 10.6084/m9.figshare.13286339).

524 **References**

- 525 1. Alvarez, L. W., Alvarez, W., Asaro, F., & Michel, H. V. Extraterrestrial cause for the
526 Cretaceous-Tertiary extinction. *Science*, **208(4448)**, 1095-1108(1980).
- 527 2. Boyden, J. A.*et al.* Next-generation plate-tectonic reconstructions using
528 GPlates(Cambridge University Press, 2011).
- 529 3. Cameron, A. G. W., & Benz, W. The origin of the Moon and the single impact
530 hypothesis IV. *Icarus*, **92(2)**, 204-216(1991).
- 531 4. Cameron, A. G., & Ward, W. R. The origin of the Moon. In *Lunar and Planetary*
532 *Science Conference (Vol. 7)*(1976).
- 533 5. Canup, R. M., &Asphaug, E. Origin of the Moon in a giant impact near the end of the
534 Earth's formation. *Nature*, **412(6848)**, 708-712(2001).
- 535 6. Connerney, J. E. P.*et al.* Magnetic lineations in the ancient crust of Mars. *Science*,
536 **284(5415)**, 794-798(1999).
- 537 7. Daly, R. A. Origin of the Moon and its topography. *Proceedings of the American*
538 *Philosophical Society*, **90(2)**, 104-119(1946).
- 539 8. ESRI (2015) [https://pro.arcgis.com/en/pro-app/help/mapping/properties/cylindrical-](https://pro.arcgis.com/en/pro-app/help/mapping/properties/cylindrical-equal-area.htm)
540 [equal-area.htm](https://pro.arcgis.com/en/pro-app/help/mapping/properties/cylindrical-equal-area.htm)
- 541 9. Evatt, G. W.*et al.* The spatial flux of Earth's meteorite falls found via Antarctic data.
542 *Geology*, **48(7)**, 683-687(2020).
- 543 10. Le Feuvre, M., &Wieczorek, M. A. Non-uniform cratering of the terrestrial planets.
544 *Icarus*, **197(1)**, 291-306(2008).
- 545 11. Li, S.S.*et al.* Anatomy of impactites and shocked zircon grains from Dhala reveals
546 Paleoproterozoic meteorite impact in the Archean basement rocks of Central India.
547 *Gondwana Research*, **54**, 81-101 (2018).

- 548 12. Flamini, E., Di Martino, M., & Coletta, A. (Eds.). *Encyclopedic Atlas of Terrestrial*
549 *Impact Craters* (Springer 2019).
- 550 13. French, B. M. 25 years of the impact-volcanic controversy: Is there anything new
551 under the Sun or inside the Earth? *Eos, Transactions American Geophysical Union*,
552 **71(17)**, 411-414 (1990).
- 553 14. French, B. M. (1998) Traces of catastrophe: A handbook of shock-metamorphic
554 effects in terrestrial meteorite impact structures 1-120 (LPI Contribution no. 954)
- 555 15. French, B. M. The importance of being cratered: The new role of meteorite impact as
556 a normal geological process. *Meteoritics & Planetary Science*, **39(2)**, 169-197 (2004).
- 557 16. French, B. M., & Koeberl, C. The convincing identification of terrestrial meteorite
558 impact structures: What works, what doesn't, and why. *Earth-Science Reviews*,
559 **98(1-2)**, 123-170 (2010).
- 560 17. Grieve, R. A. (1991) Terrestrial impact: The record in the rocks. *Meteoritics*, **26(3)**,
561 175-194.
- 562 18. Grieve, R. A. Extraterrestrial impacts on earth: the evidence and the consequences.
563 *Geological Society, London, Special Publications*, **140(1)**, 105-131 (1998).
- 564 19. Grieve, R. A. F. *Impact structures in Canada* p. 210. (Geological Association of
565 Canada 2006).
- 566 20. Grieve, R. A., & Shoemaker, E. M. The record of past impacts on Earth in *Hazards*
567 *due to comets and asteroids* (ed. Gehrels, T.) 417-462 (1994).
- 568 21. Haines, P. W. Impact cratering and distal ejecta: the Australian record. *Australian*
569 *Journal of Earth Sciences*, **52(4-5)**, 481-507 (2005).

- 570 22. Halliday, I. The variation in the frequency of meteorite impact with geographic
571 latitude. *Meteoritics*, **2(3)**, 271-278(1964).
- 572 23. Halliday, I., & Griffin, A. A. A study of the relative rates of meteorite falls on the
573 earth's surface. *Meteoritics*, **17(1)**, 31-46(1982).
- 574 24. Hartmann, W. K., & Davis, D. R. Satellite-sized planetesimals and lunar origin.
575 *Icarus*, **24(4)**, 504-515(1975).
- 576 25. Hoyt, W. G. *Coon Mountain controversies: Meteor Crater and the development of*
577 *impact theory*. (University of Arizona Press 1987).
- 578 26. Jourdan, F., Moynier, F., Koeberl, C., & Eroglu, S. $^{40}\text{Ar}/^{39}\text{Ar}$ age of the Lonar crater
579 and consequence for the geochronology of planetary impacts. *Geology*, **39(7)**, 671-
580 674(2011).
- 581 27. Keerthy, S. *et al.* Reconstructing the dimension of Dhala Impact Crater, Central India,
582 through integrated geographic information system and geological records. *Planetary*
583 *and Space Science*, **177**, 104691(2019).
- 584 28. Kresák, L. The latitude variation of the meteor shower influx. *Bulletin of the*
585 *Astronomical Institutes of Czechoslovakia*, **15**, 53(1964).
- 586 29. Mark, K. (1987) *Meteorite Craters*. University of Arizona Press, Tucson, AZ. 288.
- 587 30. Marvin, U. B. Meteorites, the Moon and the history of geology. *Journal of Geological*
588 *Education*, **34(3)**, 140-165(1986).
- 589 31. Marvin, U. B. Impact and its revolutionary implications for geology in *Global*
590 *catastrophes in earth history* 147-154 (ed. Sharpton, V. L. & Ward, P. D. 1990).
- 591 32. Marvin, U. B. Impacts from space: the implications for uniformitarian geology.
592 *Geological Society, London, Special Publications*, **150(1)**, 89-117(1999).

- 593 33. Masaitis, V. L. The Barringer Medal Address: Impact craters: Are they
594 useful? *Meteoritics*, **27(1)**, 21-27(1992).
- 595 34. Müller, R.D. *et al.* Gplates: Building a virtual earth through deep time. *Geochemistry,*
596 *Geophysics, Geosystems*. **19**, 2243-2261(2018).
- 597 35. Osinski, G. R., & Pierazzo, E. Impact cratering: Processes and products. *Impact*
598 *Cratering*, 1-20(Wiley 2013).
- 599 36. Reimold, W. U.) Impact cratering comes of age. *Science*, **300(5627)**, 1889-
600 1890(2003).
- 601 37. Reimold, W. U., Koeberl, C., Gupta, H., & Fareeduddin, F. Catastrophes, extinctions
602 and evolution: 50 years of impact cratering studies. *Golden Jubilee Memoir of the*
603 *Geological Society of India*, **66**, 69-10(2008).
- 604 38. Robbins, S. J.) A New Global Database of Lunar Impact Craters > 1–2 km: 1. Crater
605 Locations and Sizes, Comparisons with Published Databases, and Global Analysis.
606 *Journal of Geophysical Research: Planets*, **124(4)**, 871-892(2019).
- 607 39. Robbins, S. J., & Hynek, B. M. A new global database of Mars impact craters \geq 1 km:
608 1. Database creation, properties, and parameters. *Journal of Geophysical Research:*
609 *Planets*, **117(E5)**(2012).
- 610 40. Schmieder, M., & Kring, D. A. Earth's Impact Events Through Geologic Time: A List
611 of Recommended Ages for Terrestrial Impact Structures and Deposits. *Astrobiology*,
612 **20(1)**, 91-141(2020).
- 613 41. Schulte, P. *et al.* The Chicxulub asteroid impact and mass extinction at the
614 Cretaceous-Paleogene boundary. *Science*, **327(5970)**, 1214-1218(2010).

- 615 42. Scotese, C. R. PALEOMAP PaleoAtlas for GPlates and the PaleoData Plotter
616 Program, PALEOMAP Project. See [http://www.earthbyte.org/paleomap-paleoatlas-](http://www.earthbyte.org/paleomap-paleoatlas-for-gplates)
617 [for-gplates](http://www.earthbyte.org/paleomap-paleoatlas-for-gplates) (accessed 17 October 2017)(2016).
- 618 43. Sears, J. W., & Alt, D. Impact origin of large intracratonic basins, the stationary
619 Proterozoic crust, and the transition to modern plate tectonics in *Basement*
620 *Tectonics* 8 (pp. 385-392). (Springer1992).
- 621 44. Shoemaker, E. M. Asteroid and comet bombardment of the Earth. *Annual Review of*
622 *Earth and Planetary Sciences*, **11(1)**, 461-494(1983).
- 623 45. Shoemaker, E. M., & Shoemaker, C. S. Connolly Basin: a probable eroded impact
624 crater in Western Australia in *Lunar and Planetary Science Conference*.**17**, 797-
625 798(1986)
- 626 46. Sleep, N. H. Martian plate tectonics. *Journal of Geophysical Research: Planets*,
627 **99(E3)**, 5639-5655(1994).
- 628 47. Spray J.G., Kelly, S. P., & Rowley, D.B. Evidence for a late Triassic multiple impact
629 event on Earth. *Nature*, **392**,171-173(1998).
- 630 48. Telecka, M., &Matyjasek, J. Paleopositions of the chains of the meteorite craters on
631 the Earth in *AnnalesUniversitatisMariae Curie-Sklodowska*.**66(1)**, 53) (De Gruyter
632 Open Sp. zoo.2011)
- 633 49. Thackeray, S., Walkden, G.M., & Dunn, G. Geological aspects of terrestrial impact
634 cratering rates; simulating the processes and effect of crater removal in *Proceedings*
635 *of the 40th ESLAB–1st International Conference on Impact Cratering in the Solar*
636 *System*, ESA-ESTEC, Noordwijk, Netherlands, 123-127(2006).

- 637 50. Tianfeng, W., Yanhong, Y., & Changhou, Z. On the extraterrestrial impact and plate
638 tectonic dynamics: a possible interpretation. In *Comparative planetology, geological*
639 *education, history of geology: proceedings of the 30th International Geological*
640 *Congress, Beijing, China, 4-14 August 1996*. **26**, 87 (1997).
- 641 51. Wieczorek, M. A., & Le Feuvre, M. Did a large impact reorient the Moon? *Icarus*,
642 **200(2)**, 358-366(2009).

643 **List of Figures**

- 644 1. Paleo- and present position of Earth impact craters. The trail shows the
645 displacement of the craters. 174 craters that are <1100 Ma old are displayed
646 (Source of background image: [www. natureearthdata.com](http://www.natureearthdata.com)) (Maps prepared using
647 ArcGIS 10.4.1 and Paleo-positions using GPlates 2.2.0).
- 648 2. Distance and displacement undergone by the 687 Ma old Jänisjärvi impact crater
649 (Source of background image: www. natureearthdata.com)(Maps prepared using
650 ArcGIS 10.4.1 and Paleo-positions using GPlates 2.2.0).
- 651 3. The impact event with age and its latitudinal segment. Area of that particular
652 latitudinal segment at the time of impact is depicted in the column diagram. The
653 black line shows the changes in land area through 1100 Ma geological time and the
654 dot in it represent the impact event.
- 655 4. Pie diagram showing the average land area of different latitudinal segments (0-30°
656 area is for 900-0 Ma; 30-60° for 750-0 Ma and 60-90° for 602-0 Ma). The column
657 diagram represents the distribution of craters within that latitudinal segment and with
658 respect to geological time (ordinate is percentage).

659 5. Percentage of craters in each latitudinal segment for Earth (a), Moon (b) and Mars
660 (c) (Sources of backdrop image- Earth: <https://www.universetoday.com/>; Moon:
661 <https://www.space.com/>; Mars: <https://mars.nasa.gov/>)

662 **List of Tables**

- 663 1. Inventory of Earth impact crater showing diameter, age, paleo- and present
664 coordinates, paleo- and present plates, distance and displacement it has undergone
665 since its origin.
- 666 2. Latitudinal distribution of Earth impact craters.
- 667 3. Comparison of impact craters on Earth, Moon and Mars for the different latitudinal
668 segments

Figure 1.



● Present position of impact craters ● Paleo-position of impact craters — Trace of impact crater displacement

3000 km

Figure 2.

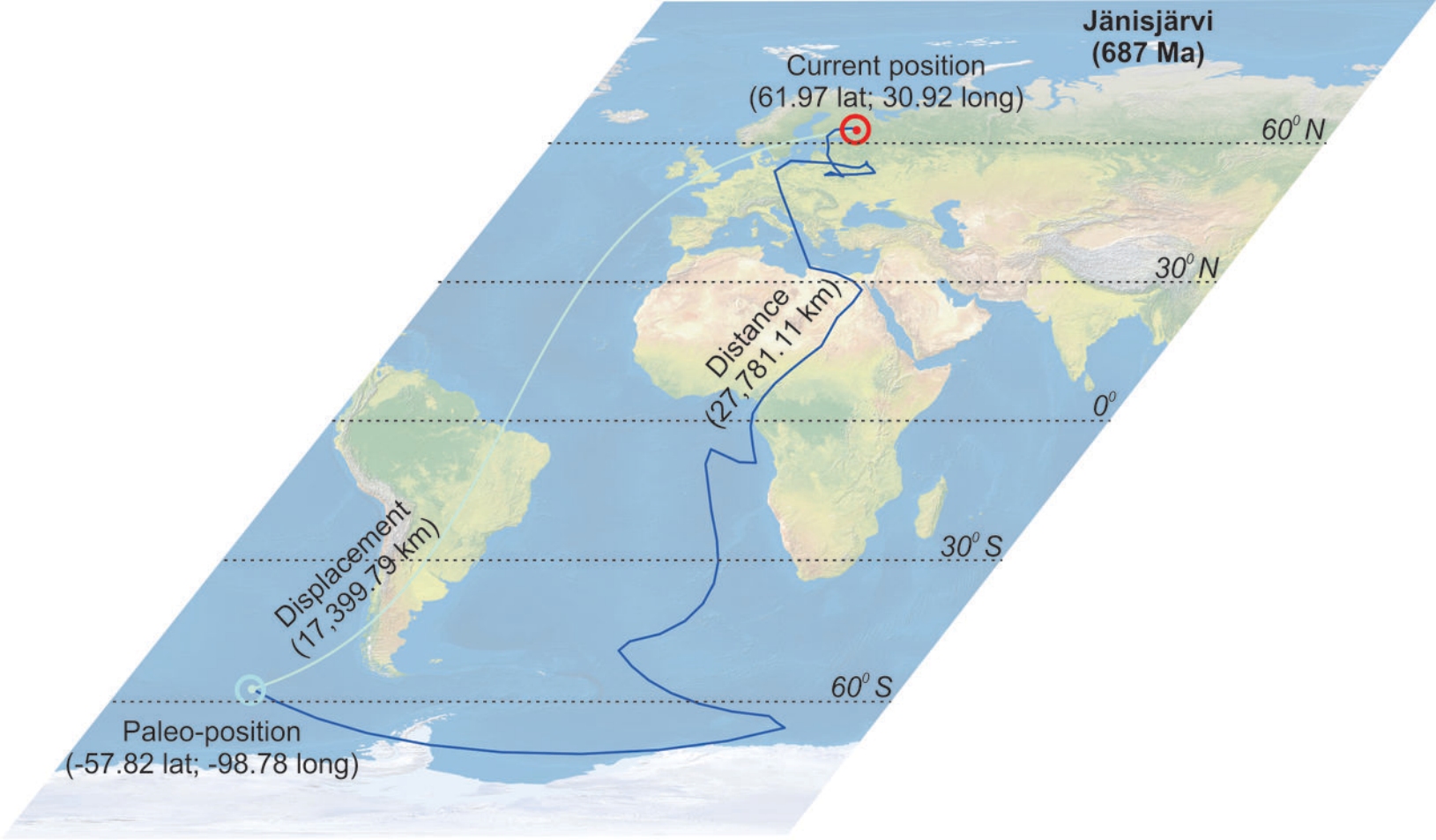


Figure 3.

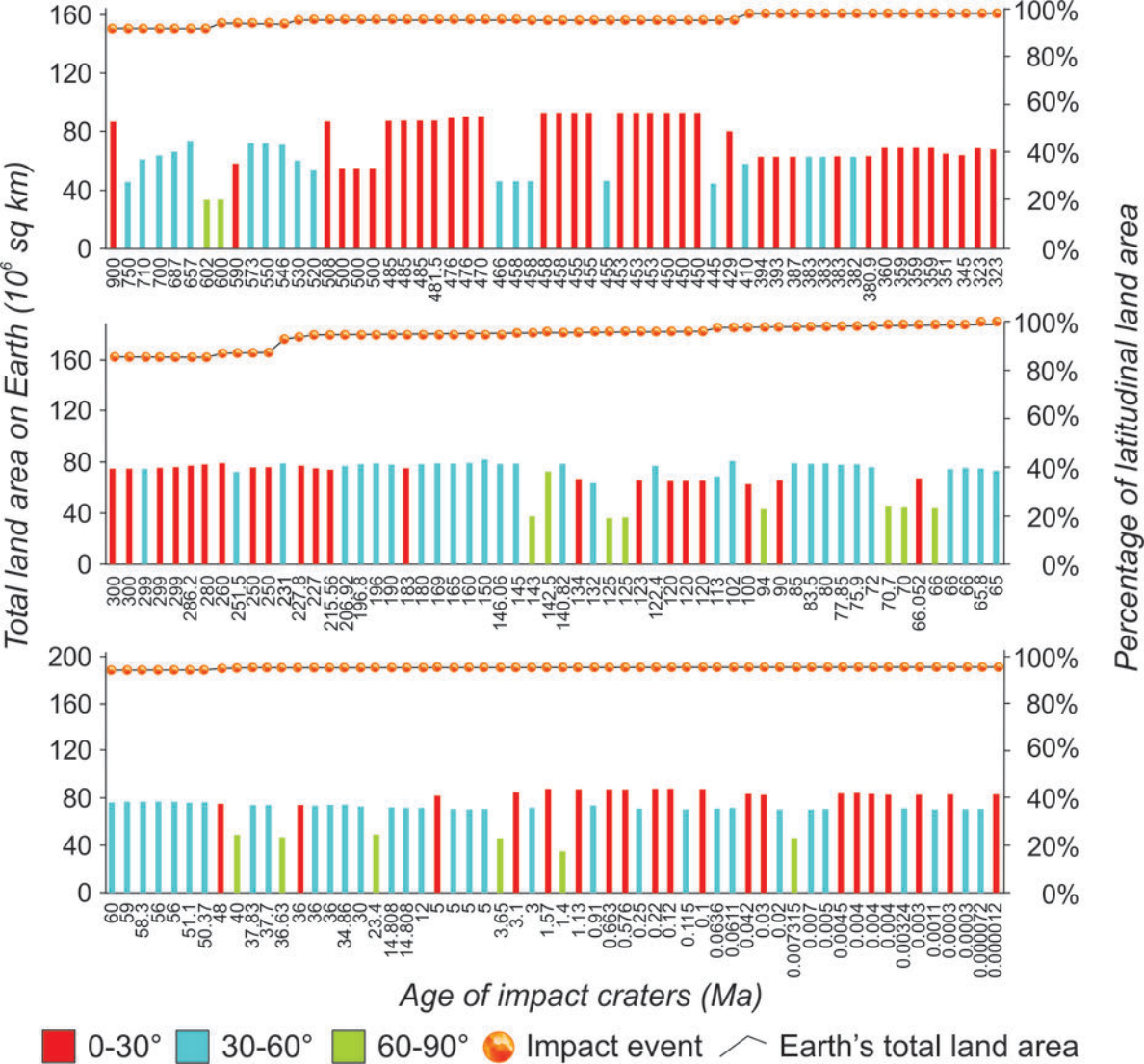
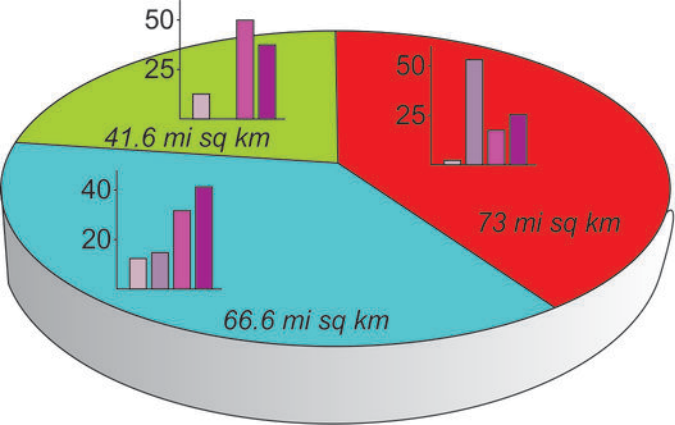
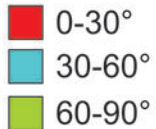


Figure 4.



Legend

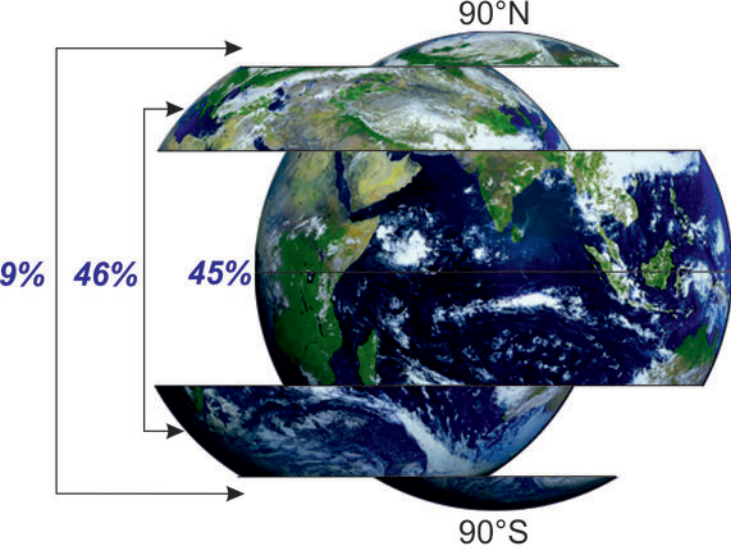
Latitudes



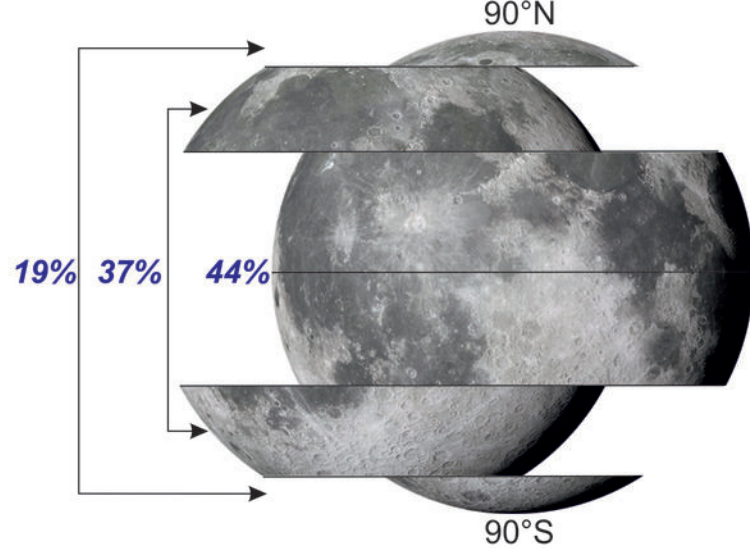
Geologic time



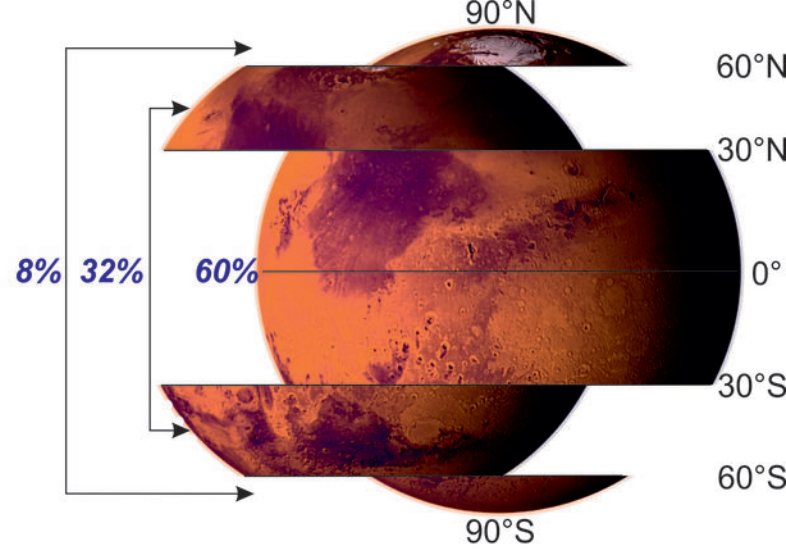
Figure 5.



(a)



(b)



(c)

Table 1 Inventory of Earth impact crater showing diameter, age, paleo- and present coordinates, paleo- and present plates, distance and displacement it has undergone since its origin

1(a)												
SI No.	Name of crater	Present Coordinates		Paleo Coordinates		Diameter (km)	Age (Ma)	Age ascertained to obtain paleoposition (Ma)	Present Continent	Palaeo Plate	Distance Travelled (km)	Displacement (km)
		Latitude	Longitude	Latitude	Longitude							
1	Beaverhead	44.60	-113.00	-14.48	-166.25	60	900-470	900	North America	Eastern Basin and Range	39289.44	8467.53
2	Ramgarh	25.33	76.62	38.35	150.35	10	~750-165	750	Asia	Indian Craton	34781.57	6944.90
3	Suvasvesi South	62.59	28.21	-47.15	-111.63	3.8	710	710	Europe	Northern European Craton and Eurasia	29049.88	16987.59
4	Spider	-16.74	126.08	48.70	-162.90	13	700	700	Australia	Australia	30648.55	10062.85
5	Jänisjärvi	61.97	30.92	-57.82	-98.78	14	687±5	687	Asia	Northern European Craton and Eurasia	27781.11	17399.79
6	Strangways	-15.20	133.58	45.73	-160.56	25	657±43	657	Australia	Australia	30061.48	9434.53
7	Sääksjärvi	61.41	22.38	-66.43	2.93	6	602±17	602	Europe	Northern European Craton and Eurasia	22157.92	14270.45
8	Saarijärvi	65.29	28.39	-62.72	13.41	1.5	<600-520	600	Europe	Northern European Craton and Eurasia	22229.02	14254.54

Table 2 Latitudinal distribution of Earth impact craters

<i>Sl. No</i>	<i>Crater</i>	<i>Optimum Age</i>	<i>Paleo-latitude</i>	<i>Latitudinal Segment (degree)</i>	<i>Total land area on Earth (sq. km)</i>	<i>Land Area at segment (sq. km)</i>	<i>Latitudinal land area: Total land area</i>
1	Beaverhead	900	-14.47977	0 - 30	150822000	79449771.58	0.53
2	Ramgarh	750	38.354821	30 - 60	150747700	41344488.96	0.27
3	Suvasvesi South	710	-47.148474	30 - 60	150893900	54716479.65	0.36
4	Spider	700	48.697584	30 - 60	150930000	57177834.07	0.38
5	Jänisjärvi	687	-57.818	30 - 60	150974400	59951241.09	0.4
6	Strangways	657	45.725044	30 - 60	150974400	66464619.2	0.44
7	Sääksjärvi	602	-66.426342	60 - 90	151119200	29884525.5	0.2
8	Saarijärvi	600	-62.722825	60 - 90	154362700	31108415.89	0.2

Table 3 Comparison of impact craters on Earth, Moon and Mars for the different latitudinal segments

<i>Latitudinal Segments</i>	Earth				Moon			Mars		
	<i>Ratio of latitudinal area to total area</i>	<i>Normalized ratio</i>	<i>No of Craters</i>	<i>% of crater</i>	<i>Ratio of latitudinal area to total area</i>	<i>No of Craters</i>	<i>% of crater</i>	<i>Ratio of latitudinal area to total area</i>	<i>No of Craters</i>	<i>% of crater</i>
0°-30°	0.4309	0.4182	78	45	0.5607	576155	44.43	0.5781	231912	60.34
30°-60°	0.3726	0.3616	80	46	0.3635	479174	36.95	0.3490	122997	32.00
60°-90°	0.2269	0.2202	16	9	0.0758	241467	18.62	0.0729	29434	7.66
TOTAL	1.0304	1.0000	174		1.0000	1296796		1.0000	384343	

o